

Supplementary Figures

Single-cell transcriptomics reveal extracellular vesicles secretion with a cardiomyocyte proteostasis signature during pathological remodeling

Eric Schoger^{1,2,3*}, Federico Bleckwedel^{1,2*}, Giulia Germena^{4,2}, Cheila Rocha⁴, Petra Tucholla^{1,2}, Izzatullo Sobitov^{1,2}, Wiebke Möbius⁵, Maren Sitte⁶, Christof Lenz^{7,8}, Mostafa Samak^{4,2}, Rabea Hinkel^{4,2,9}, Zoltán V. Varga^{10,11}, Zoltán Giricz^{10,11}, Gabriela Salinas⁶, Julia C. Gross¹² and Laura C. Zelarayán^{1,2,3}

*The authors contributed equally

¹ Institute of Pharmacology and Toxicology, University Medical Center Göttingen (UMG), 37075 Göttingen, Germany

² German Center for Cardiovascular Research (DZHK) partner site Göttingen, 37075 Göttingen, Germany

³ Cluster of Excellence "Multiscale Bioimaging: from Molecular Machines to Networks of Excitable Cells" (MBExC), University of Göttingen, 37075 Göttingen, Germany

⁴ Laboratory Animal Science Unit, Leibniz-Institut für Primatenforschung, Deutsches Primatenzentrum GmbH, 37075 Göttingen, Germany

⁵ Max-Planck-Institute for Multidisciplinary Sciences, 37075 Göttingen, Germany

⁶ NGS Integrative Genomics Core Unit (NIG), University Medical Center Göttingen (UMG), 37075 Göttingen, Germany

⁷ Department of Clinical Chemistry, University Medical Center Göttingen (UMG), 37075 Göttingen, Germany

⁸ Bioanalytical Mass Spectrometry Group, Max Planck Institute for Multidisciplinary Sciences, 37075 Göttingen, Germany

⁹ Institute for Animal Hygiene, Animal Welfare and Farm Animal Behaviour (ITTN), Stiftung Tierärztliche Hochschule Hannover, University of Veterinary Medicine, 30173 Hannover, Germany.

¹⁰ HCEMM-SU Cardiometabolic Immunology Research Group, Department of Pharmacology and Pharmacotherapy, Semmelweis University, H-1085 Budapest, Hungary

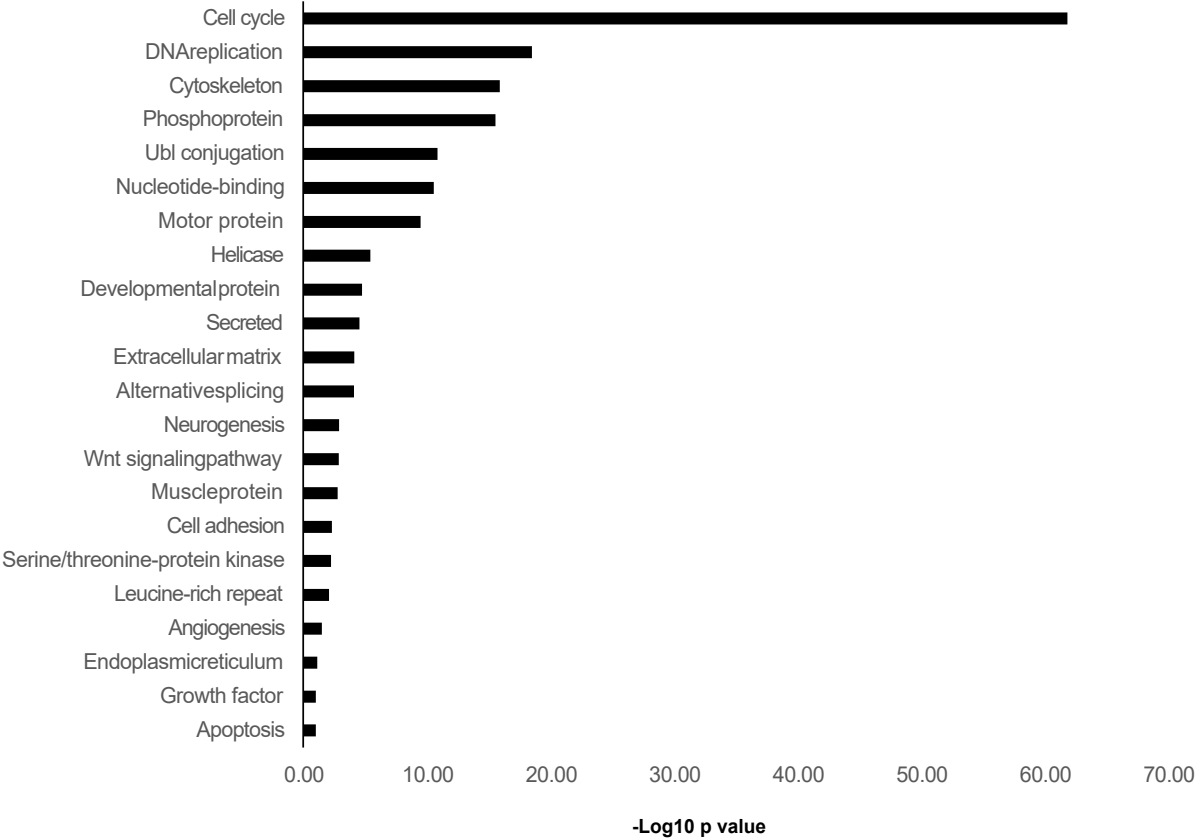
¹¹ Pharmahungary Group, H-1085 Budapest, Hungary

¹² Health and Medical University, D-14471 Potsdam, Germany

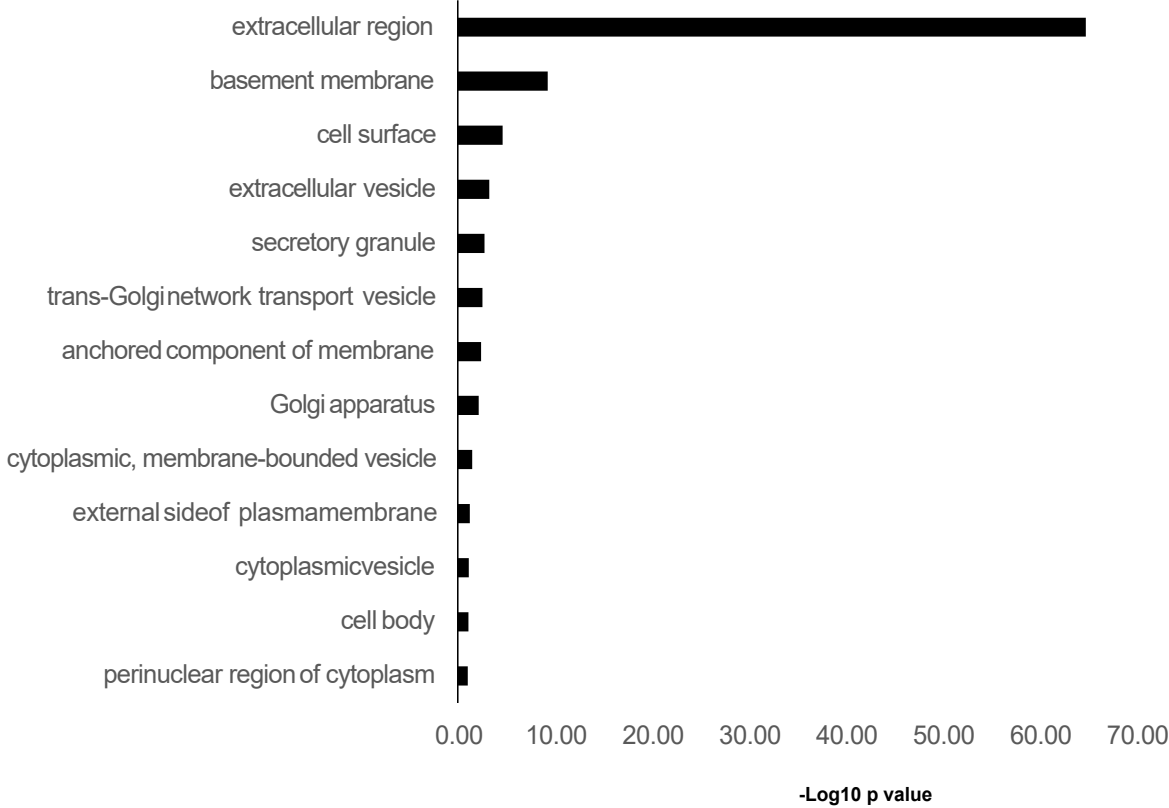
Corresponding Author: Laura C. Zelarayán, laura.zelarayan@med.uni-goettingen.de

Supplementary Figure 1

a GO Molecular function of upregulated transcript in β -cat Δ ex3 hearts versus control

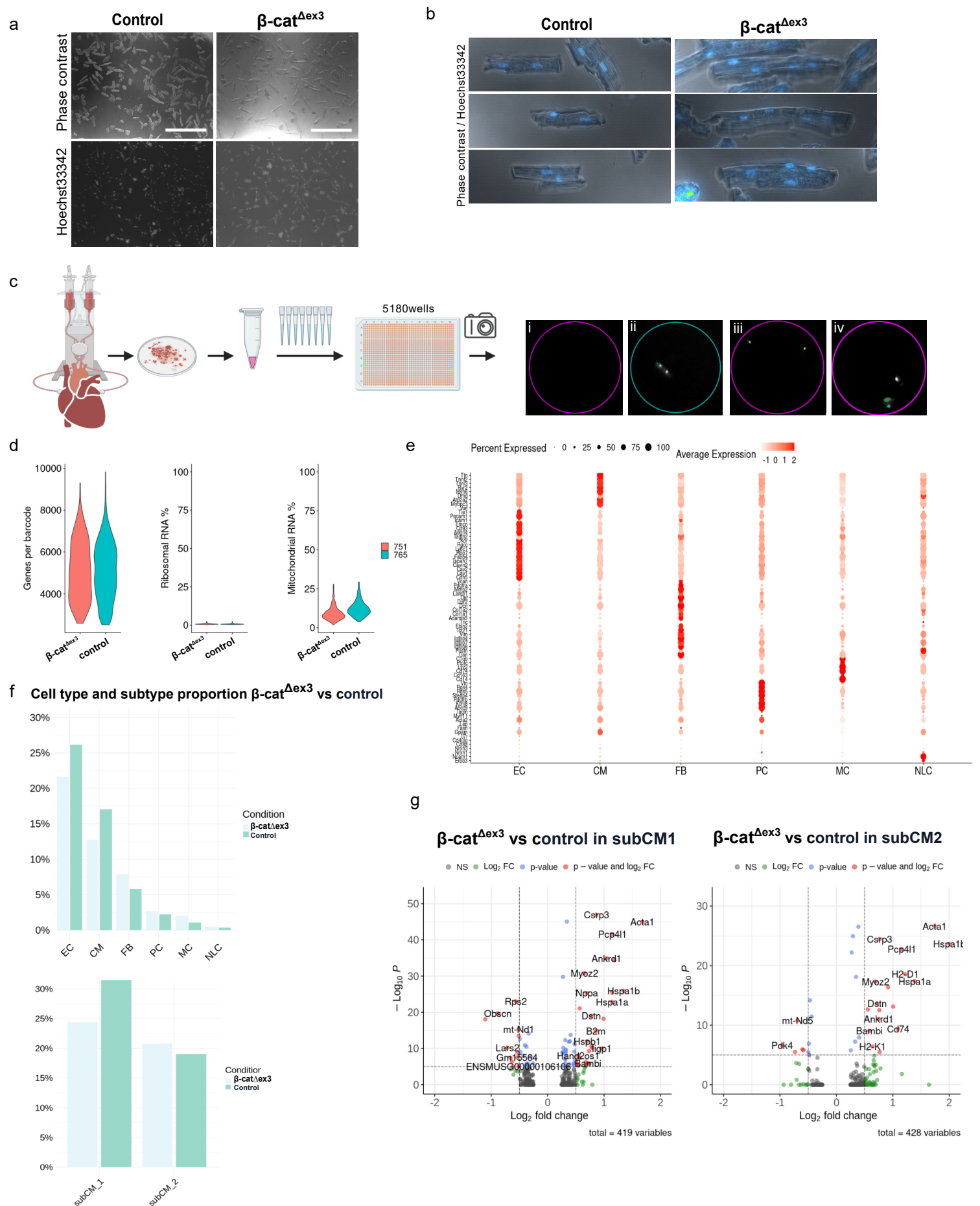


b GO Cellular compartments of genes clustering in secreted, ECM and membrane processes in A for β -cat Δ ex3 hearts



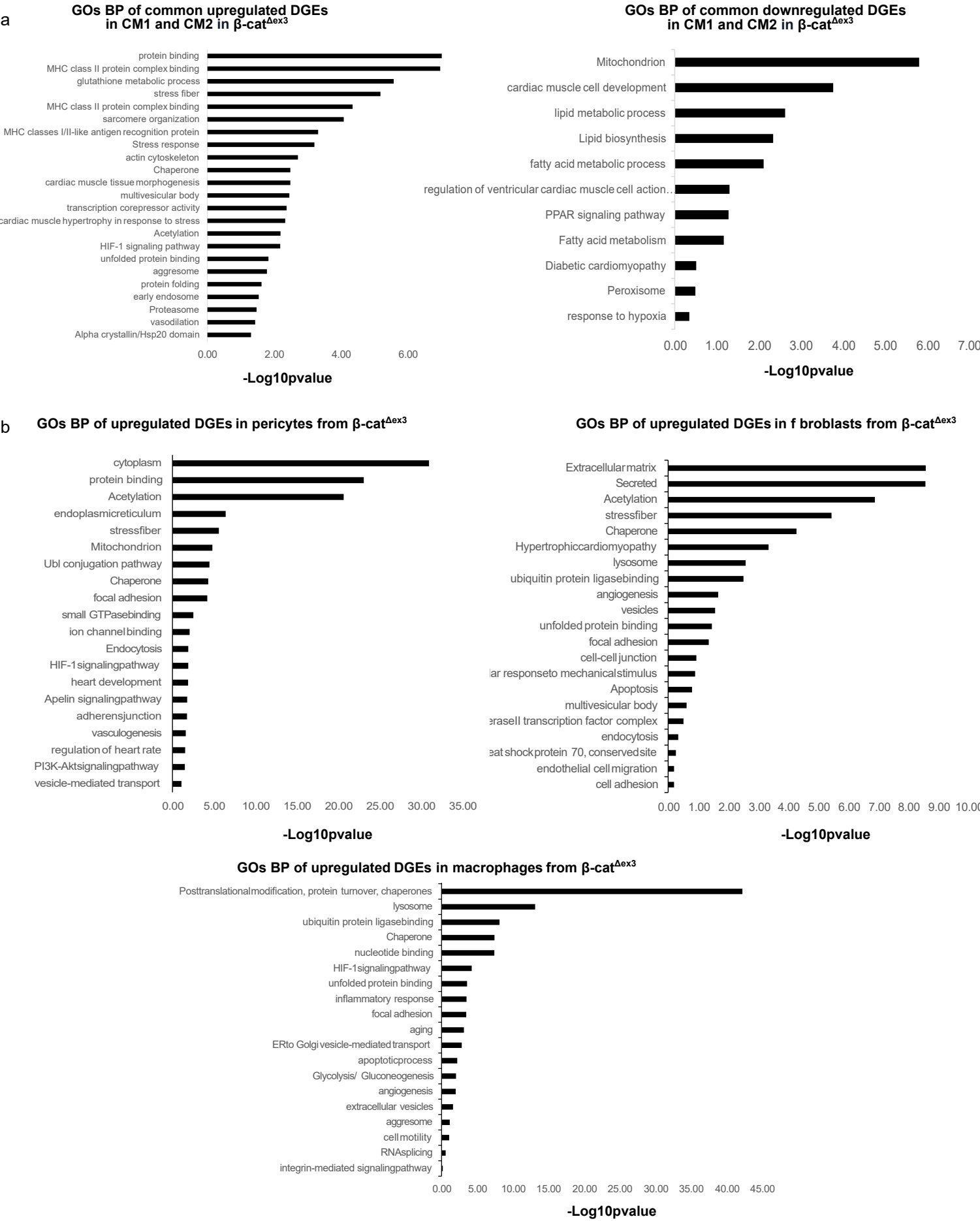
a. Selected top categories from gene ontology (GO) cellular compartments processes enrichment of upregulated DEGs in β -cat Δ ex3 versus control hearts from bulk RNAseq data. **b.** Selected top categories from GO molecular function of genes clustering to membrane based processes and secreted proteins in **a.** $-\log_{10}$ p value (p value <0.05), term fusion was applied.

Supplementary Figure 2



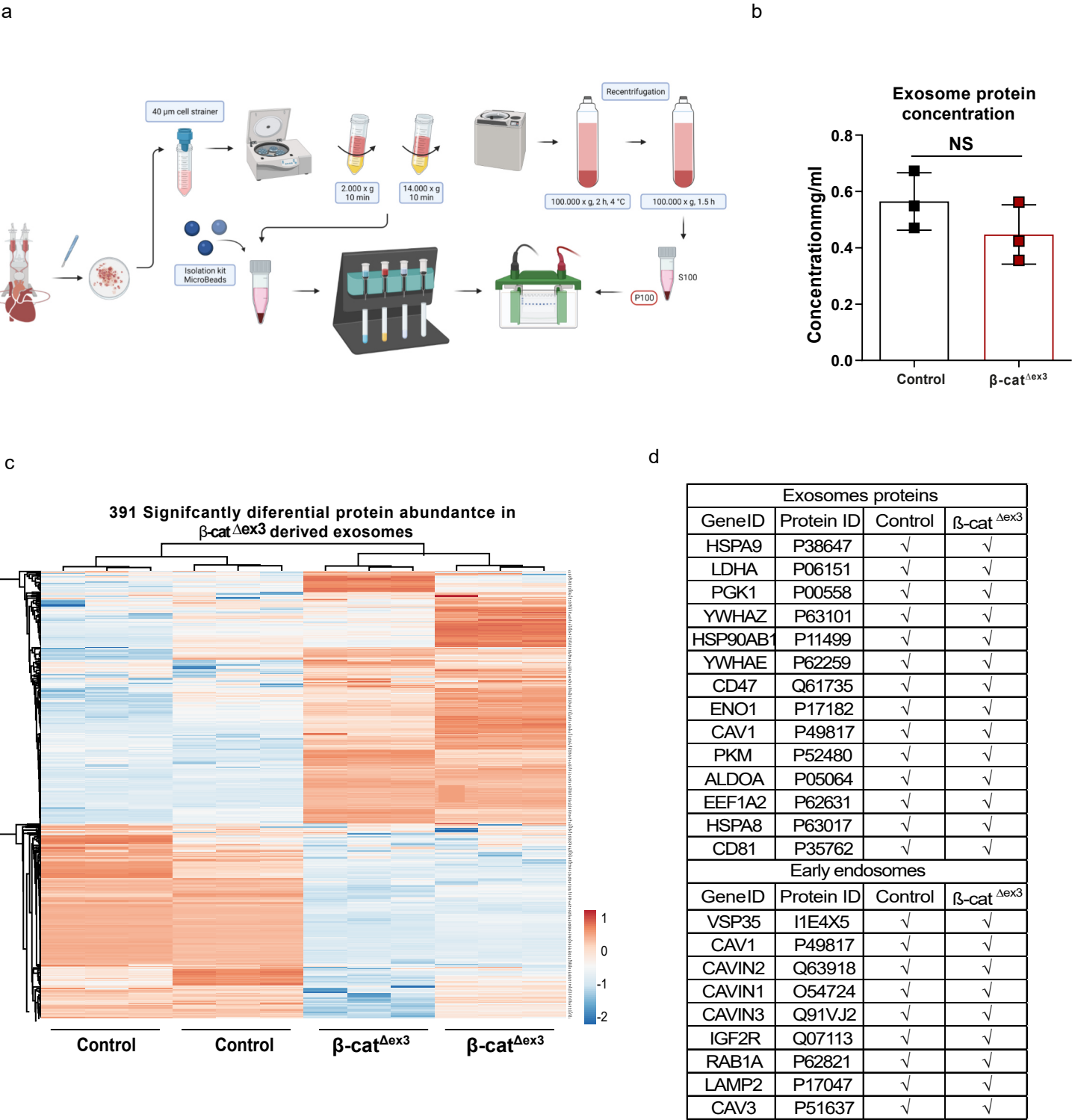
a. Isolated cardiac cells from Langendorff perfused hearts including rod-shaped cardiomyocytes and **(b)** hypernucleated, hypertrophic cardiomyocytes from β -cat $^{\Delta ex3}$ hearts compared to control. Scale bar = 20 μ m. **c.** Schematic overview of cardiac cell isolation and distribution into nanowells for single cell transcriptome analyses using the iCell8 system. Cells are dissociated and dispensed into a 5180 well plate for library preparation and sequencing. The wells contained no cells (i), single multinucleated cells (ii), two cells (iii) or death cells (iv). Only cells as represented in ii were considered for sequencing. **d.** Quality control assessment of single cell transcripts analysed per heart indicating a mean of 4,5K and 4,4K genes per barcode (cell) in β -cat $^{\Delta ex3}$ and control samples respectively. In addition, low presence of ribosomal and mitochondrial contamination was confirmed. **e.** Dot plots showing different marker gene expression used to cluster cell-types according to known and reported cell markers. **f.** Distribution of cells in the different conditions (control or β -cat $^{\Delta ex3}$ hearts) as well as the distribution of the CM1 and CM2 subclusters. **g.** Volcano plot comparing DEGs in CM1 and CM2 β -cat $^{\Delta ex3}$ versus control hearts.

Supplementary Figure 3



Selected top categories from gene ontology (GO) biological processes (BP) enrichment of common upregulated (left) and downregulated (right) DEGs in CM1 and CM2 (a) and in macrophage, fibroblast and pericyte clusters (b) of β -cat ^{Δ ex3} versus control hearts. GO enrichment represents $-\log_{10}$ p-value (p-value <0.05) and term fusion was applied.

Supplementary Figure 4

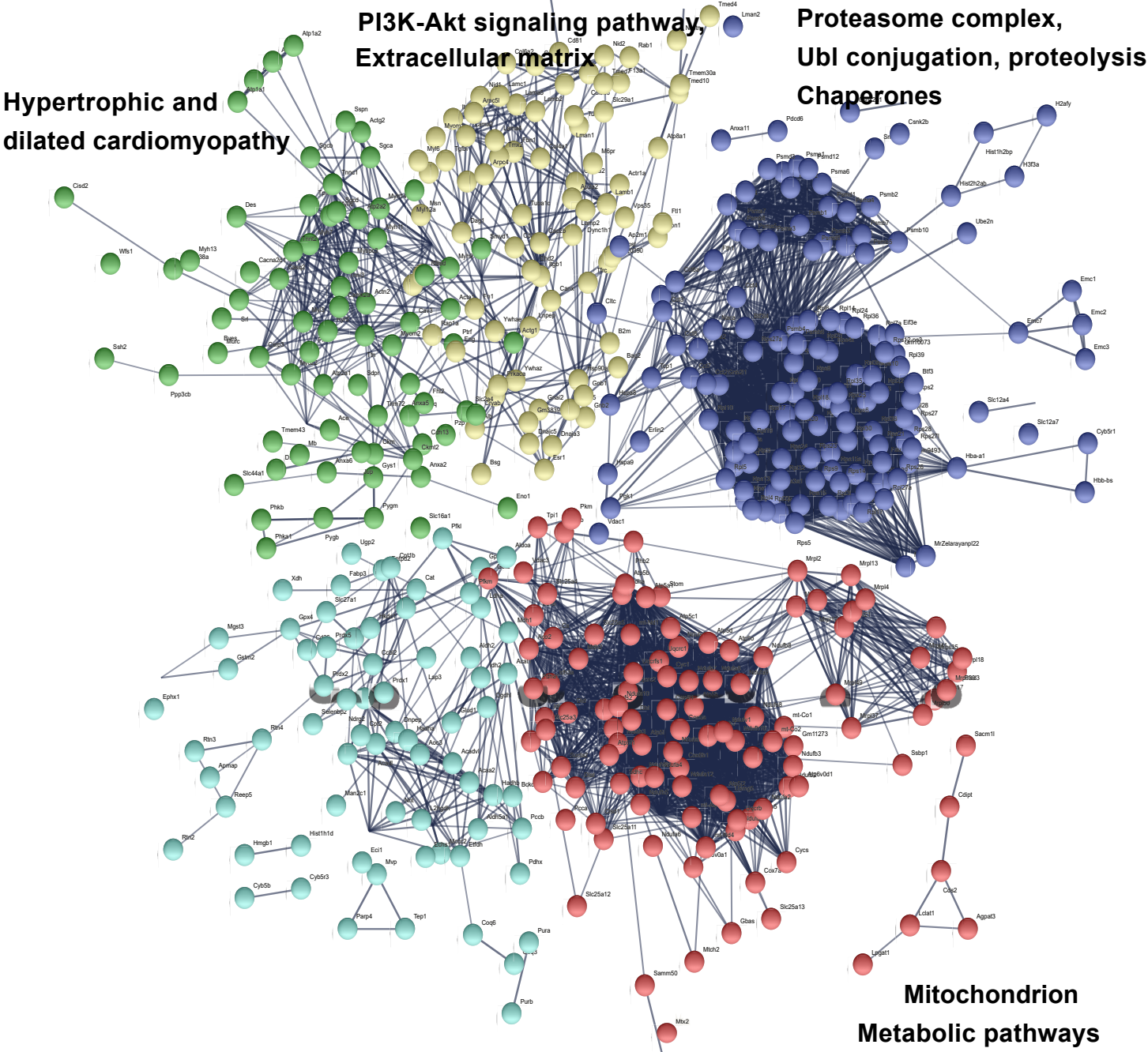


a. Overview of exosome isolation procedure from adult mouse hearts by UC and magnetic bead-based purification (Created with BioRender.com). **b.** Total protein concentration was comparable in exosome preparations regardless of experimental group (β -cat^{Δex3} and control). **c.** Heat-map of significantly enriched proteins (391) in β -cat^{Δex3} cardiac derived exosomes compared to controls. **d.** Classical exosomal and early endosomal proteins were identified enriched proteins.

Supplementary Figure 5

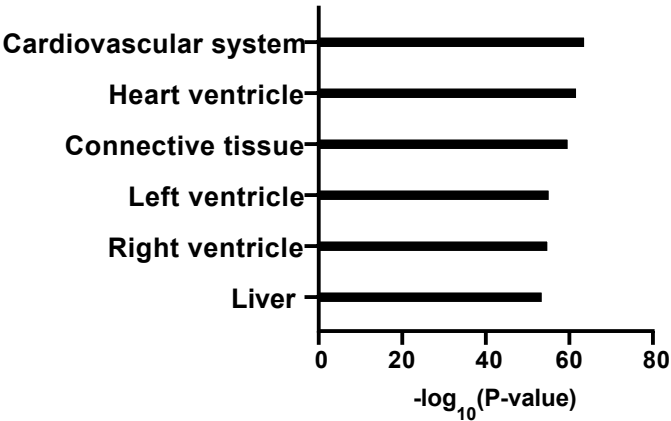
a

Clustering of total detected proteins



b

GO: Tissue expression

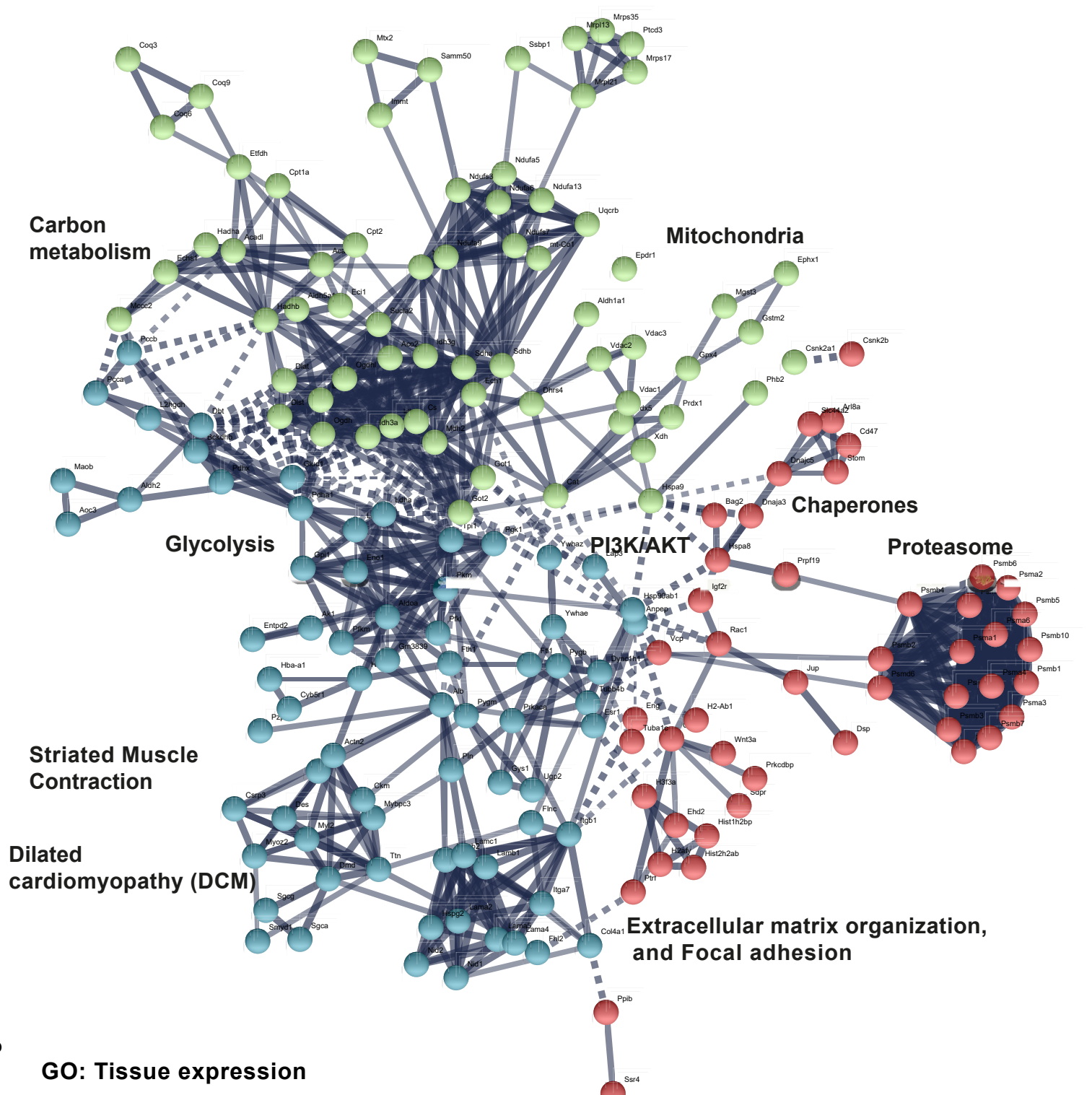


a. STRING analyses derived networks of protein-protein interactions of the total mass spectrometry data (573 proteins) revealed subclusters of protein classes with distinct cellular functions characteristic for EVs. **b.** The identified proteins categorized to the cardiovascular system in a tissue enrichment analysis. GO enrichment represents $-\log_{10}$ was considered for sequencing and term fusion was applied.

Supplementary Figure 6

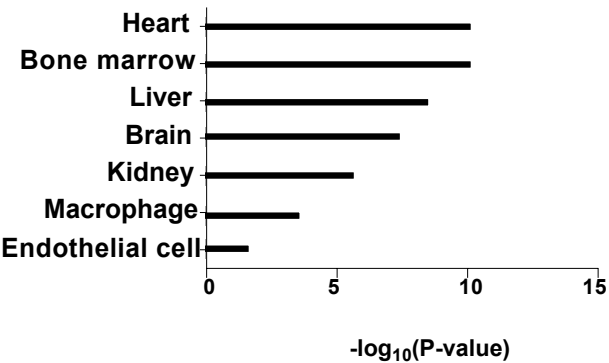
a

Clustering of proteins enriched in β -cat ^{Δ ex3} isolated cardiac exosomes



b

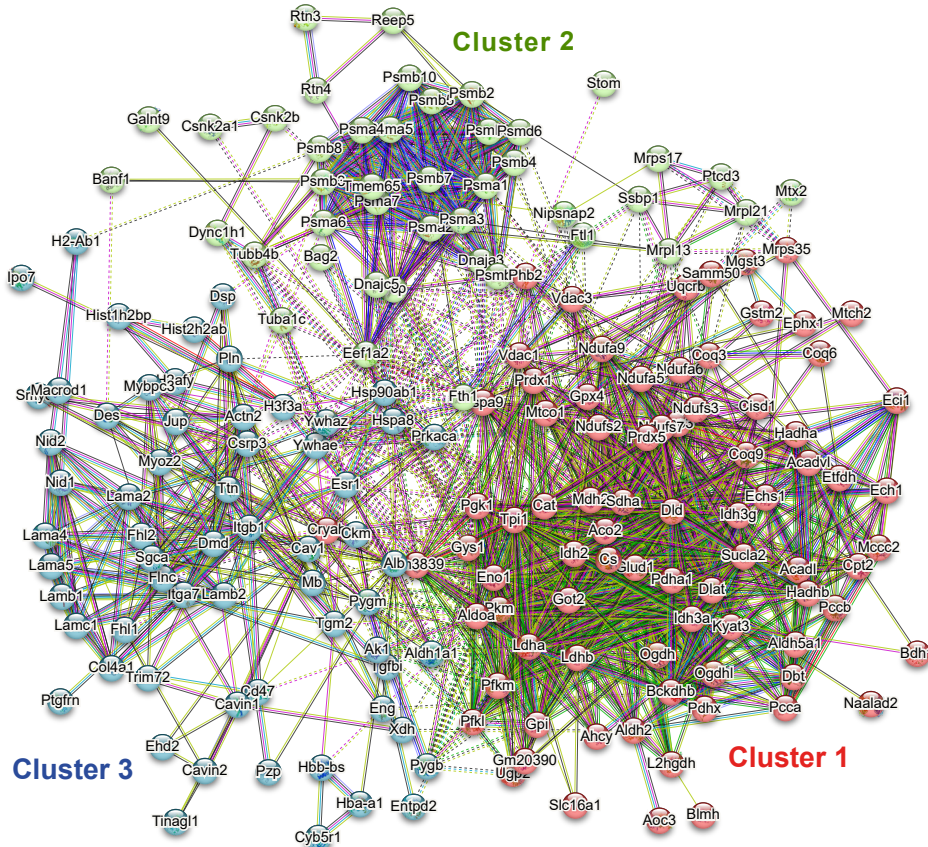
GO: Tissue expression



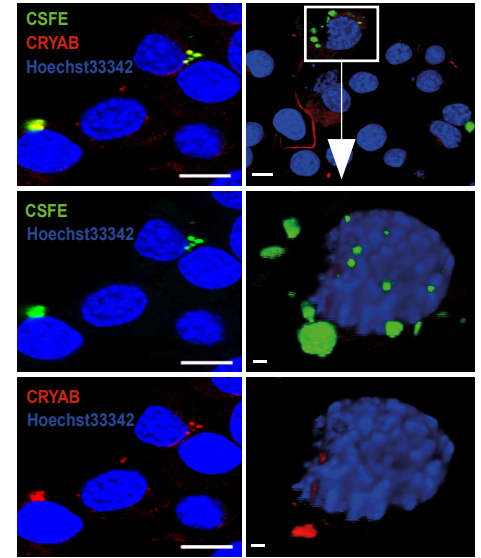
a. STRING analyses derived networks of protein-protein interactions of the enriched proteins (391) in β -cat ^{Δ ex3} cardiac derived extracellular vesicles (EVs) compared to controls revealed sub-clusters of protein classes with distinct cellular functions characteristic for EVs. The identified proteins categorized to cardiovascular system in a tissue enrichment analysis. GO enrichment represents $-\log_{10}$ p-value (p-value < 0.05) and term fusion was applied.

Supplementary Figure 7

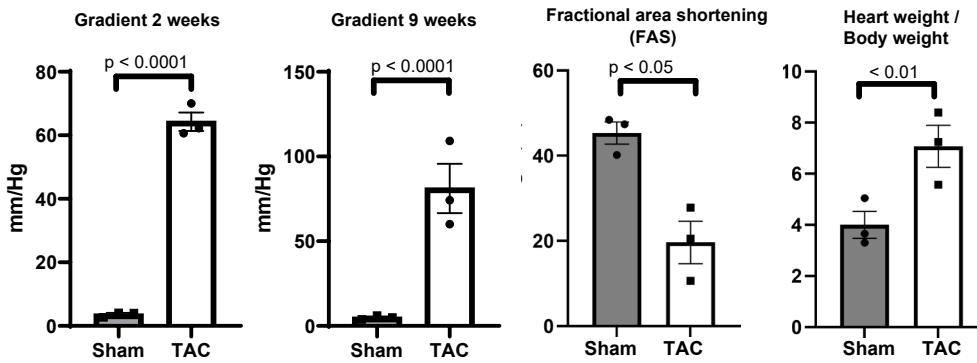
a



b



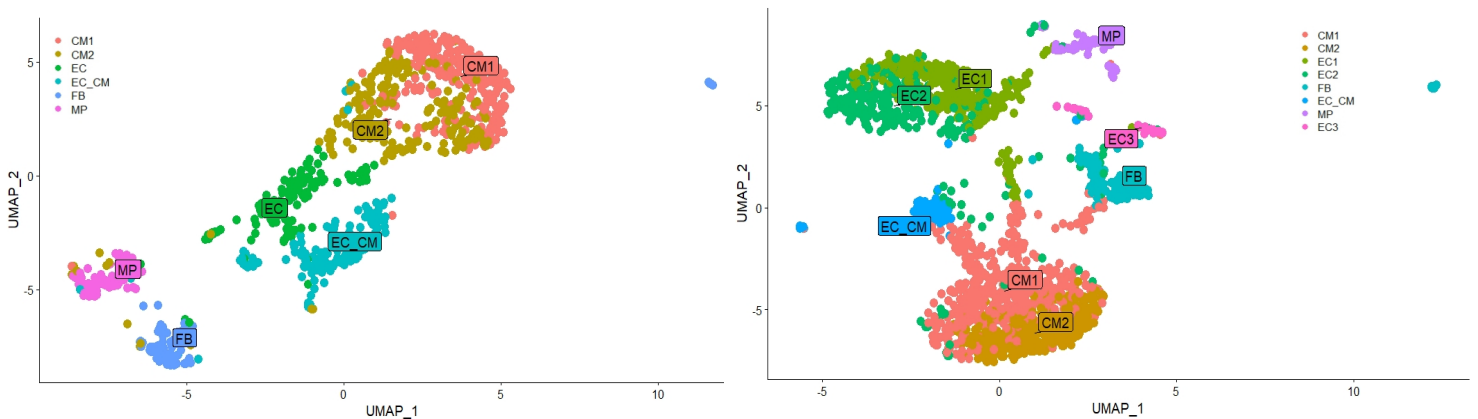
c



d

Early (compensatory) hypertrophic hearts

Late (failing) hypertrophic hearts

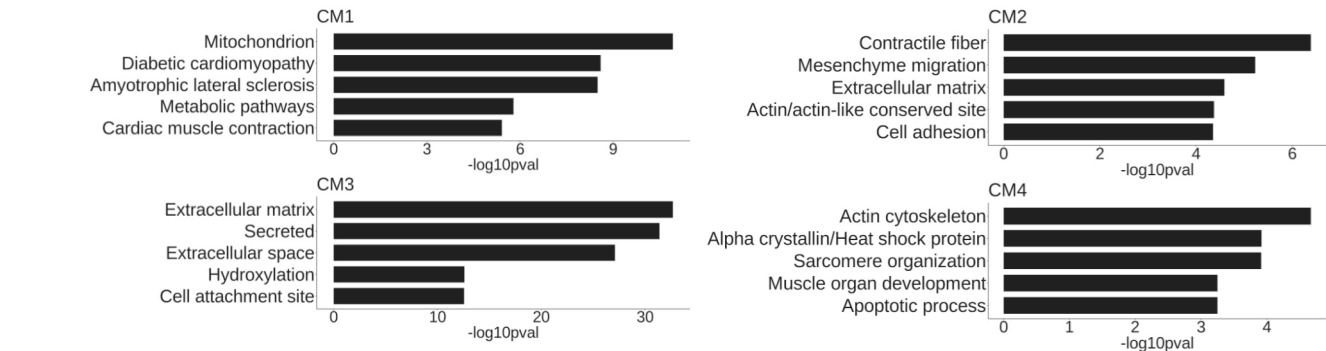


a. Cluster analysis using STRING functional annotation protein interaction database on the predicted enriched 391 proteins in exosomes from β -cat^{Δex3} tissue using the K-means algorithm. They were summarized into three ontological clusters (cluster 1, 2 and 3). **b.** Representative confocal images of immunofluorescence staining of N2A neuroblastoma cells that were exposed to carboxyfluorescein succinimidyl ester (CSFE)-ex vivo labelled extracellular vesicles (EVs) from β -cat^{Δex3} hearts and stained with CRYAB (n=3, technical replicates). Hoechst33342 was used for nucleus visualization. By Z-scanning we observed that CRYAB co-localized with CFSE-labelled exosomes attached to the cell surface. Scale bar = 20 μ m. **c.** Doppler-echo gradient confirming successful transverse aortic constriction with induced afterload increase upon intervention compared to sham in early- and late-stage disease condition. **d.** Fractional area shortening (FAS) was reduced upon TAC and heart weight normalized to body weight was elevated. Data are shown as mean \pm SEM; t-test. **d.** UMAP plot after scRNA-seq and data integration of cardiac cells isolated from healthy (sham) and disease (TAC) hearts of CH (left) and FH (right) depicting the different cell clusters.

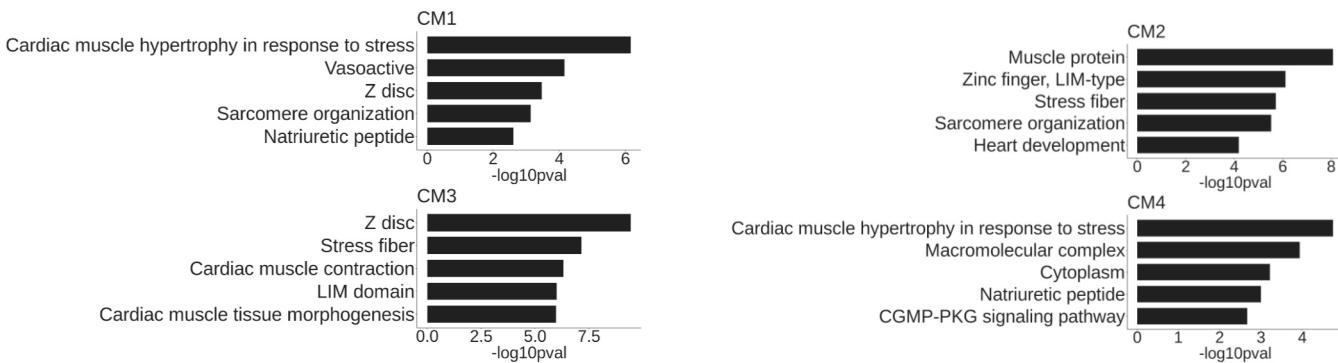
Supplementary Figure 8

a

GO: BP of upregulated DEGs in CM sub-clusters in compensatory hypertrophy

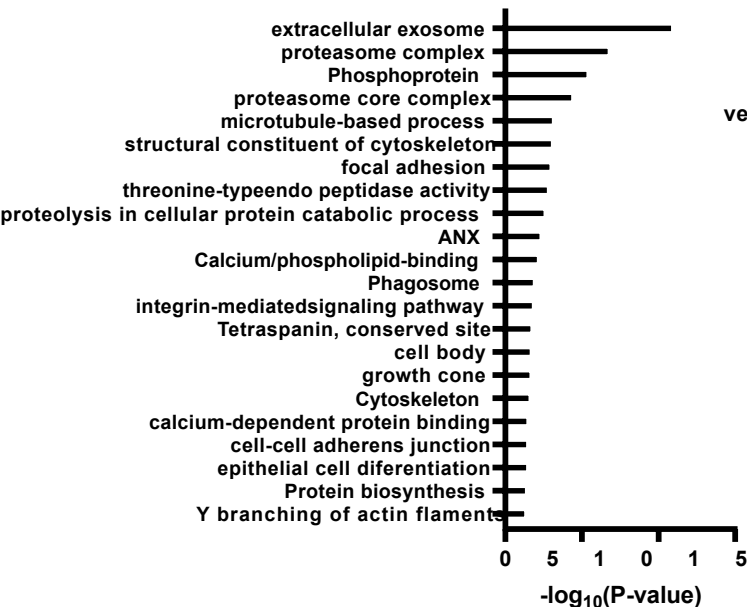


GO: BP of upregulated DEGs in CM sub-clusters in failing hypertrophy

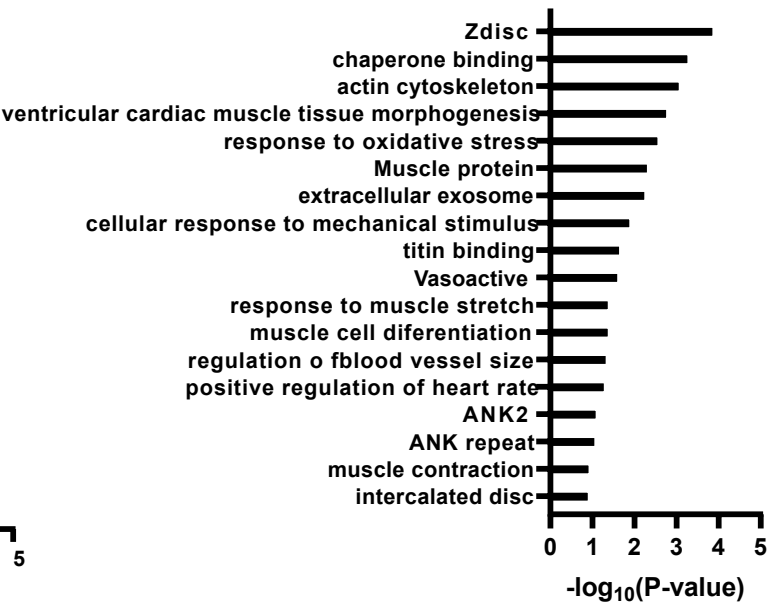


b

GO: BP of intersercted DEGs from TAC vs sham at CH with $\beta\text{-cat}^{\Delta\text{ex}3}$



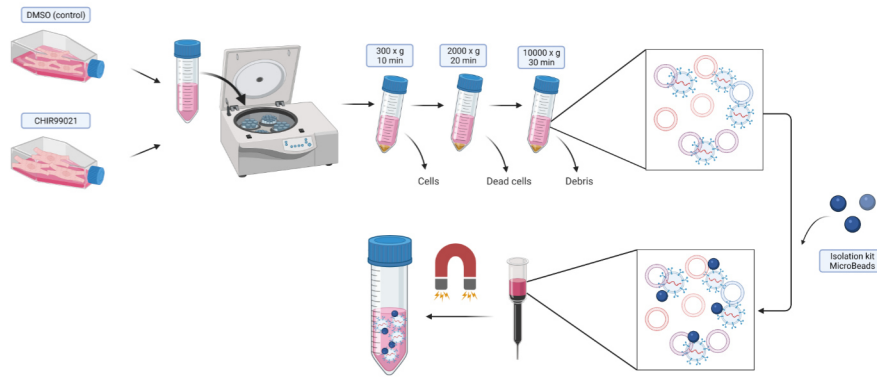
GO: BP of intersercted DEGs from TAC vs sham at FH with $\beta\text{-cat}^{\Delta\text{ex}3}$



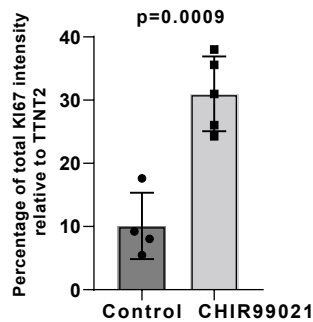
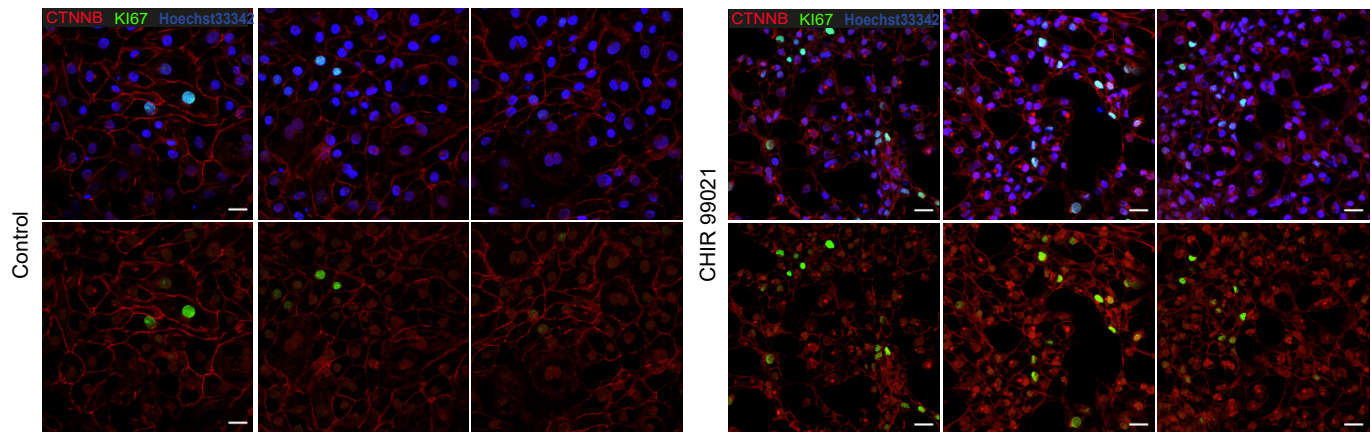
a. Selected top categories from gene ontology (GO) biological processes (BP) enrichment of upregulated DEGs in the different cardiomyocyte subclusters (CM1-CM4) from healthy (sham) and disease (TAC) hearts of compensatory and failing hypertrophy depicting the main transcriptional changes. **b.** Selected top categories from GO BP enrichment of overlapping upregulated DEGs in cardiomyocytes from TAC (versus sham) and $\beta\text{-cat}^{\Delta\text{ex}3}$ (versus control) of CH (left) and FH (right) depicting the main overlapping transcriptional changes at early and late disease states. GO enrichment represents $-\log_{10}$ p-value (p value <0.05) and term fusion was applied.

Supplementary Figure 9

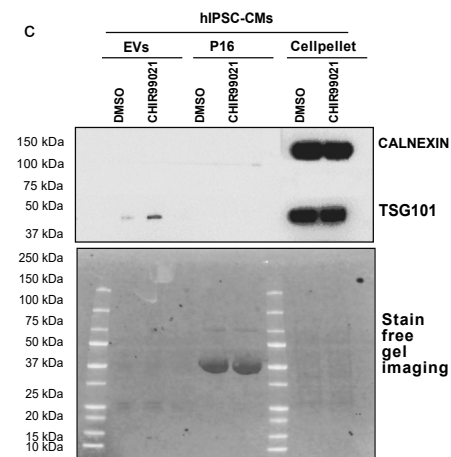
a



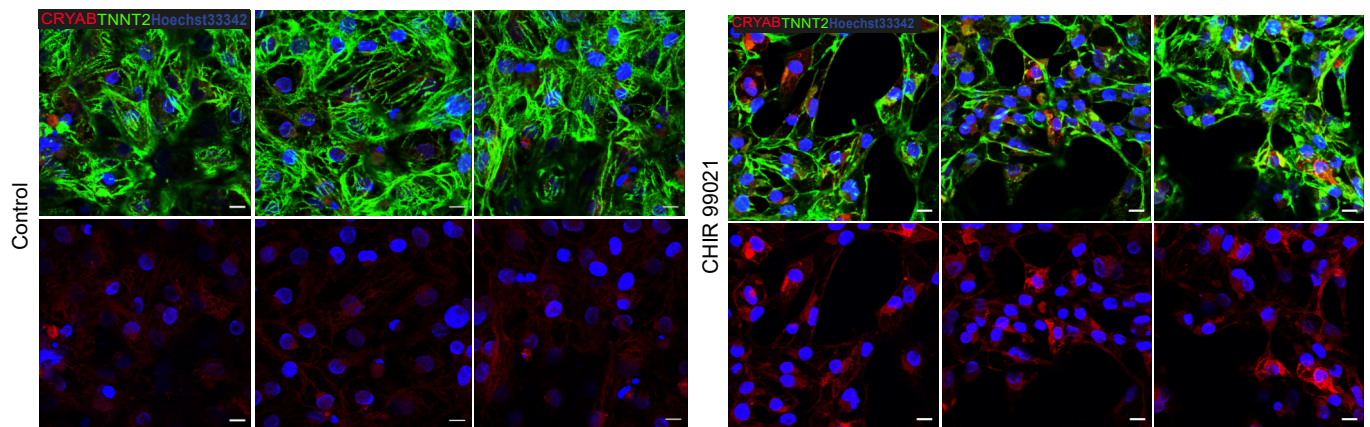
b



c



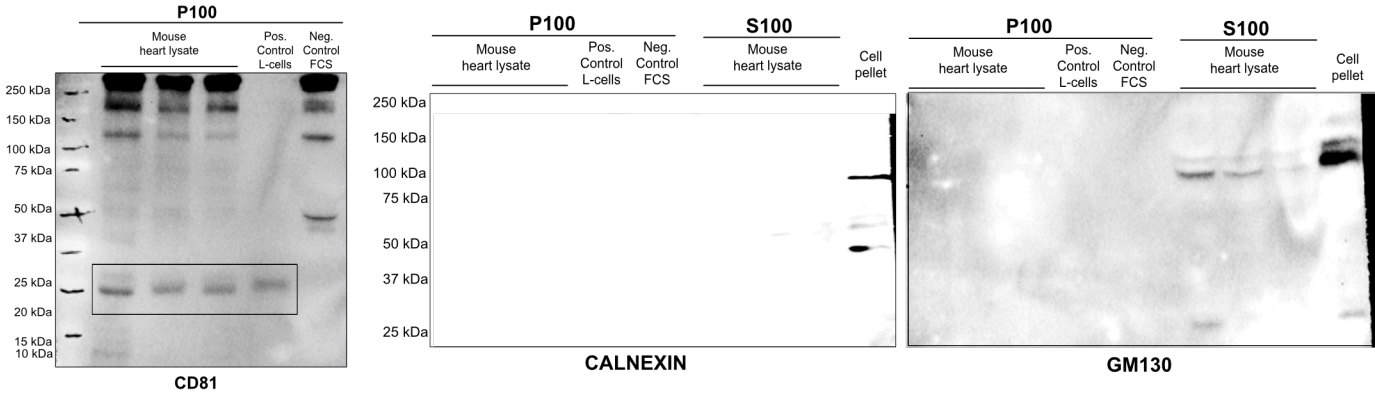
d



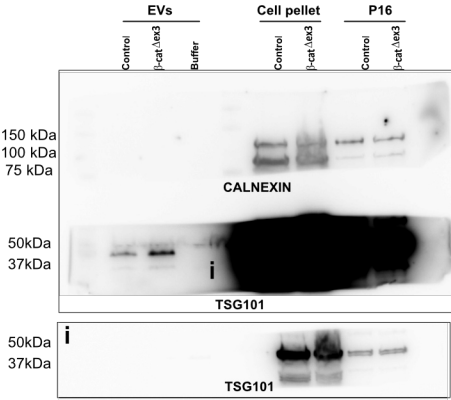
a. Schematic overview of extracellular vesicles (EVs) isolated from induced hiPSC-derived cardiomyocytes upon treatment with CHIR99021 (Wnt activated) or DMSO (control) using a magnetic bead-based protocol (n=9, technical replicates, biological duplicates) (Created with BioRender.com). **b.** Representative confocal images of immunofluorescence analysis showing increased cell cycle activity as assessed by Ki67 staining and corresponding semiquantification in CHIR99021 treated hiPSC-derived cardiomyocytes versus control DMSO. (n=3, technical replicates). Scale bar = 20 μ m. **c.** Western blot showing increased exosomal marker TSG101 as well as the absence of endoplasmic reticulum marker Calnexin in EVs from CHIR99021 treated hiPSC-derived cardiomyocytes. Calnexin was clearly detected in the cell pellet. Stain free gel showed equally amount of loaded proteins. **d.** Representative confocal images of immunofluorescence analysis showing CRYAB accumulation in CHIR99021 treated hiPSC-derived cardiomyocytes versus control DMSO. (n=3, technical replicates). Scale bar = 20 μ m. Data are shown as mean \pm SEM; unpaired student's t-test.

Supplementary Figure 10

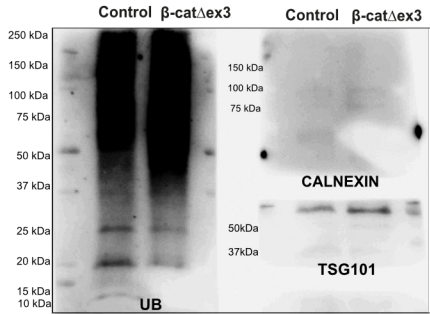
a



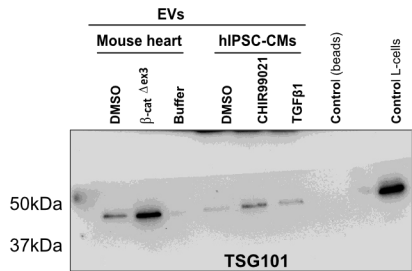
b



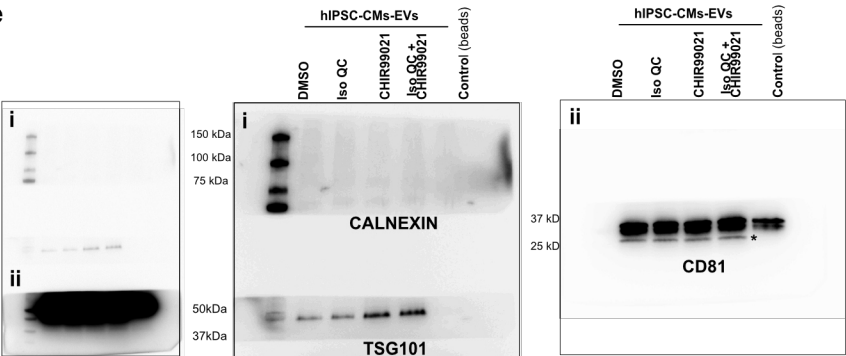
c



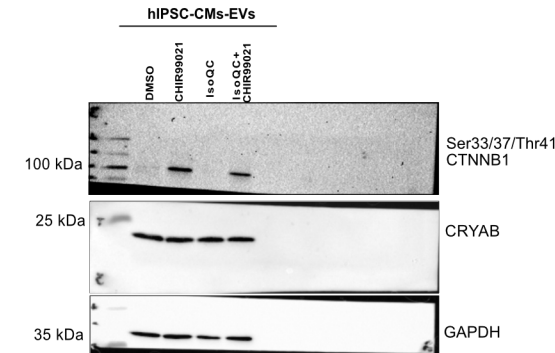
d



e



f



Whole blots used for the main figures in this study. **a**. Blots for Fig 2C. **b**. Blots for Fig 2D. (i, depicted below showing a reduced exposure time for TSG101). **c**. Blots for Fig 4A. **d**. Blots for Fig 7B. **e**. Blots for Fig 7D (i, shows an increased exposure time for Calnexin and TSG101 and ii, shows an reduced exposure time for CD81). **f**. Blots for Fig 7E.